NRC Research Press

ARTICLE

# PML isoform expression and DNA break location relative to PML nuclear bodies impacts the efficiency of homologous recombination

Kathleen M. Attwood, Jayme Salsman, Dudley Chung, Sabateeshan Mathavarajah, Carter Van Iderstine, and Graham Dellaire

**Abstract:** Promyelocytic leukemia nuclear bodies (PML NBs) are nuclear subdomains that respond to genotoxic stress by increasing in number via changes in chromatin structure. However, the role of the PML protein and PML NBs in specific mechanisms of DNA repair has not been fully characterized. Here, we have directly examined the role of PML in homologous recombination (HR) using I-SceI extrachromosomal and chromosome-based homology-directed repair (HDR) assays, and in HDR by CRISPR/Cas9-mediated gene editing. We determined that PML loss can inhibit HR in an extrachromosomal HDR assay but had less of an effect on CRISPR/Cas9-mediated chromosomal HDR. Overexpression of PML also inhibited both CRISPR HDR and I-SceI-induced HDR using a chromosomal reporter, and in an isoform-specific manner. However, the impact of PML overexpression on the chromosomal HDR reporter was dependent on the intranuclear chromosomal positioning of the reporter. Specifically, HDR at the *TAP1* gene locus, which is associated with PML NBs, was reduced compared with a locus not associated with a PML NB; yet, HDR could be reduced at the non-PML NB-associated locus by PML overexpression. Thus, both loss and overexpression of PML isoforms can inhibit HDR, and proximity of a chromosomal break to a PML NB can impact HDR efficiency.

*Key words:* PML, PML nuclear bodies, homologous recombination, CRISPR/Cas9, homology-directed repair.

**Résumé :** Les corps nucléaires PML (PML NB) sont des sous-domaines nucléaires qui répondent au stress génotoxique en croissant en nombre au moyen de changements de la structure de la chromatine. Toutefois, le rôle de la protéine PML et des PML NB dans des mécanismes spécifiques de réparation d'ADN n'ont pas été complètement caractérisés. Les auteurs ont examiné directement le rôle de PML dans la recombinaison homologue (HR) à l'aide de tests de réparation dirigée par homologie (HDR) extrachromosomique et chromosomique induite par I-SceI et dans la HDR par édition génique médiée par CRISPR/Cas9. Ils ont démontré que la perte de PML peut inhiber la HR lors d'un test de HDR extrachromosomique, mais avait un effet moindre sur la HDR chromosomique médiée par CRISPR/Cas9. La surexpression de PML inhibait aussi la HDR médiée par CRISPR/Cas9 et la HDR induite par I-Sce I sur un rapporteur chromosomique, de manière spécifique à l'isoforme. Toutefois, l'impact de la surexpression de PML sur le rapporteur de HDR chromosomique était dépendant du positionnement chromosomique intranucléaire du rapporteur. Particulièrement, la HDR sur le locus génique *TAP1*, qui est associé aux PML NB, était réduite comparativement à un locus non associé à un PML NB; néanmoins, la HDR pouvait être réduite sur le locus non associé à un PML NB par la surexpression de PML. Ainsi, tant la perte que la surexpression des isoformes de PML peuvent inhiber la HDR, et la proximité d'un bris chromosomique à un PML NB peut affecter l'efficacité de la HDR. [Traduit par la Rédaction]

*Mots-clés :* PML, corps nucléaires PML, recombinaison homologue, CRISPR/Cas9, réparation dirigée par homologie.

## Introduction

Promyelocytic leukemia nuclear bodies (PML NBs) are proteinaceous nuclear subdomains that are present in most mammalian cell lines and tissues. PML NBs range in size between 0.1–1.0 μm and typically number between 5 and 30 bodies per nucleus, depending on tissue and cell type, cell cycle phase, and differentiation stage (Dellaire and Bazett-Jones 2004; Lallemand-Breitenbach and de The 2010). Many proteins (in the range of >100) are known to be recruited to PML NBs, associating either constitutively or transiently (Dellaire et al. 2003; Boden et al. 2010). As such, PML NBs are structurally dynamic and functionally heterogeneous subnuclear domains. Owing to the diversity of associated proteins, PML NBs have been implicated in a wide range of cellular functions, including induction of apoptosis, activation of cell cycle checkpoints and senescence, transcriptional regulation, antiviral responses, protein degradation and post-translational modification, chromosome positioning, coordination of the DNA damage response, and DNA repair (Dellaire and Bazett-Jones 2004; Ching et al. 2005; Bernardi and Pandolfi 2007; Everett and Chelbi-Alix 2007; Chang et al. 2018; Lallemand-Breitenbach and de The 2018).

The primary structural component of PML NBs is the PML protein itself. PML is not essential for cell survival; however, PML-null mice display an increased risk of tumor development, and decreased PML expression has been linked to tumor progression in several cancer types, all of which may be tied to the diverse tumor-

Received 11 April 2019. Accepted 24 October 2019.

**K.M. Attwood.** Department of Biochemistry & Molecular Biology, Dalhousie University, Halifax, NS B3H 4R2, Canada.
**J. Salsman, D. Chung, S. Mathavarajah, and C. Van Iderstine.** Department of Pathology, Dalhousie University, Halifax, NS B3H 4R2, Canada.
**G. Dellaire.** Department of Biochemistry & Molecular Biology, Dalhousie University, Halifax, NS B3H 4R2, Canada; Department of Pathology, Dalhousie University, Halifax, NS B3H 4R2, Canada.
**Corresponding author:** Graham Dellaire (email: dellaire@dal.ca).

suppressing roles of PML NBs (Wang et al. 1998; Salomoni and Pandolfi 2002; Gurrieri et al. 2004; Trotman et al. 2006; Haupt et al. 2013). The *PML* gene is composed of 9 exons that are alternatively spliced to produce 7 isoforms (PMLI-VII) (Fagioli et al. 1992; Jensen et al. 2001). All isoforms share an N terminus, but vary in the central and C-terminal regions, differences that confer each isoform with specific protein-binding capabilities (Jensen et al. 2001). Upon individual PML isoform expression in *PML*$^{-/-}$ cells, PML NBs vary in size and in composition, demonstrating that isoform-specific sequences are responsible for contacting specific nuclear components to influence body formation and biochemical structure (Fagioli et al. 1992; Beech et al. 2005; Condemine et al. 2006; Weidtkamp-Peters et al. 2008; Li et al. 2017). However, the identity of exact PML isoform interaction partners, as well as the cellular function of each individual isoform in processes such as DNA repair, remains poorly understood (Condemine et al. 2006; Chang et al. 2018).

PML NBs are proteinaceous in nature and in general do not contain nucleic acids (Boisvert et al. 2000). However, studies using electron microscopy have demonstrated that PML NBs make extensive contact with chromatin fibers at their periphery (Eskiw et al. 2004). These chromatin contacts are mediated through protein-based threads emanating from the body core, and are important for maintaining both the positional stability and structural integrity of PML NBs in the nucleus (Eskiw et al. 2004; Lallemand-Breitenbach and de The 2010). Owing to the intimate association of PML bodies with chromatin, PML nuclear body number and structural integrity are highly sensitive to any topological changes in chromatin structure, such as those occurring during S-phase of the cell cycle (Dellaire et al. 2006*a*). Similarly, alterations in chromatin structure resulting from various genotoxic stresses like heavy metals, and DNA-damaging agents such as etoposide and UV have all been demonstrated to cause dispersal of PML NBs into numerous PML microbodies (Nefkens et al. 2003; Seker et al. 2003; Dellaire and Bazett-Jones 2004; Dellaire et al. 2006*b*; Kepkay et al. 2011). As such, we postulated that PML NBs may represent subnuclear sensors of cellular stress, monitoring the topological state and integrity of chromatin and releasing and (or) sequestering appropriate protein factors, and (or) aiding in their post-translational modification in response to stress (Dellaire and Bazett-Jones 2004; Dellaire et al. 2006*b*, 2009). In particular, along with the increase in body number and subcellular distribution observed following DNA damage, several lines of evidence have pointed to PML and PML NBs playing a role in the DNA damage response (DDR) via association with DNA repair factors (Dellaire and Bazett-Jones 2004; Chang et al. 2018). For example, the early DNA repair response factor MRE11 localizes at PML NBs during the DDR, possibly in response to (or to facilitate) its post-translational modification by the arginine-methyltransferase PRMT1 (Boisvert et al. 2005*a*, 2005*b*). This pattern of sequestration and post-translational modification of DDR proteins at PML NBs is a common finding, and may serve as a useful paradigm in understanding the general role of PML NBs in the DDR (Dellaire and Bazett-Jones 2004). However, in addition to playing a passive role in the response to genotoxic stress, it is now becoming increasingly clear that PML and PML NBs may be playing a role in facilitating specific pathways of DNA double-strand break (DSB) repair (Chang et al. 2018). This has come from observations that following damage, PML NBs often partially colocalize with DNA repair foci (cytological accumulations of DNA repair factors at sites of DNA DSBs) as well as with regions of single-stranded DNA (ssDNA) associated with the ssDNA-binding factor RPA1 and active DNA repair (Boe et al. 2006; Dellaire et al. 2006*b*). PML NBs have also been associated with the homologous recombination (HR) factor BRCA1, and loss of PML impairs the localization of RAD51 to repair foci following DSB induction (Boichuk et al. 2011; Yeung et al. 2012; Munch et al. 2014). Additionally, PML$^{-/-}$ cells display high rates of sister chromatid exchange (Zhong et al. 1999). Together, these findings imply that PML and (or) PML NBs may play a regulatory role in homologous recombination (HR), which is one of the major pathways of DNA DSB repair (Wyman and Kanaar 2006; Ceccaldi et al. 2016). Despite these observations, the extent to which HR is dependent on the PML protein itself or PML NBs is not fully understood, nor have the individual contributions of specific PML isoforms to HR been characterized. Here we demonstrate that both PML loss and isoform overexpression has a negative impact on HR DNA repair by both I-SceI restriction enzyme-induced homology-directed repair (HDR) and CRISPR/Cas9-mediated HDR. Furthermore, we determined that proximity of the DNA break with respect to a PML NB can impact HR efficiency and that the negative impact of PML isoform overexpression on HR is affected by the proximity of the DNA DSB to a PML NB. Thus, both loss and gain of PML expression can inhibit HR-repair and that the proximity of the DNA break within chromatin to a PML NB can impact the efficiency of homology-dependent DNA DSB repair.

## Materials and methods

### Plasmid reagents

Individual PML isoforms were cloned into p3xFLAG-CMV-10 mammalian expression vector (Sigma). Plasmids used for the Clover-Lamin homologous recombination reporter assay include pX330-U6-Chimeric_BB-CBh-hSpCas9n(D10A) (gift from Feng Zhang; Addgene #42230) (Cong et al. 2013) and piRFP670-N1 as a transfection control (gift from Vladislav Verkhusha; Addgene #45457) (Shcherbakova and Verkhusha 2013), as well as pX330-LMNAgRNA1 (Addgene plasmid #122507) and pCR2.1 CloverLMNA-donor (Addgene plasmid #122508), as described in Pinder et al. 2015. pHPRT-DRGFP (Addgene plasmid # 26475) (Pierce et al. 2001) and pCBASceI (Addgene plasmid # 26477) (Richardson et al. 1998) were a gift from Maria Jasin.

### Cell culture and generation of cell lines

Human U2OS osteosarcoma cells were obtained from ATCC (ATCC HTB-96). PML knock-out (U2OS ΔPML) was generated using two pX335-U6-Chimeric_BB-CBh-hSpCas9n(D10A) plasmids (gift from Feng Zhang; Addgene #42335) (Cong et al. 2013) each encoding Cas9D10A nickase and a guide RNA targeting the human *PML* gene near the start codon (pX335-PMLgRNA1 and pX335-PMLgRNA2) (Supplementary data, Fig. S1[1]). TERT-immortalized normal human diploid fibroblasts (NHDF) were generated from GM05757 cells as described in Kepkay et al. (2011). For the NHDF ΔPML cells, disruption of the *PML* gene was achieved by knocking-in a puromycin resistance cassette into exon 1 of the *PML* gene. The same PML-targeting sgRNAs were used as described above for U2OS cells, with the exception that a homology repair template was co-transfected with the pX335 plasmids, which contained a puromycin resistance cassette flanked by homology arms amplified from NHDF genomic DNA around PML exon 1 (Supplementary data, Figs. S2 and S3[1]). All NHDF lines derived from GM05757 cells were maintained in α-MEM supplemented with 15% fetal bovine serum (FBS; ThermoFisher Scientific) and 1% penicillin–streptomycin (ThermoFisher Scientific) at 37 °C with 5% $CO_2$. Fn1

U2OS Chr15 HR and U2OS TAP1 HR cell lines were constructed by CRISPR-mediated targeting of the direct repeats – green fluorescent protein (DR-GFP) HDR reporter derived from pHPRT-DRGFP (described in Pierce et al. 2001) to a 2079-bp intergenic region of chromosome 15 (GRCh37.p.13 primary assembly chr15: 74696007-74698086) or a 1552-bp region around exon 1 of the

[1]Supplementary data are available with the article through the journal Web site at http://nrcresearchpress.com/doi/suppl/10.1139/bcb-2019-0115.

human *TAP1* gene (GRCh37.p.13 primary assembly chr6:32821893-32823445), respectively. Full details of the generation of these cell lines are described in Supplementary data, Figs. S4–S8[1]. Human osteosarcoma U2OS cell lines [parental U2OS, U2OS ΔPML (PML knock-out), U2OS Chr15 HR, and U2OS TAP1 HR] were cultured in Dulbecco's modified Eagle's medium (DMEM; Sigma) supplemented with 10% FBS (ThermoFisher Scientific) and 1% penicillin–streptomycin (ThermoFisher Scientific) at 37 °C with 5% $CO_2$. Chr15 HR and TAP1 HR cells were also maintained in 1 μg/mL puromycin.

**Western blotting**

Antibodies used for Western blotting analysis were: rabbit anti-PML (A301–167A, 1:2000; Bethyl Laboratories), which reacts with all PML isoforms; mouse anti-actin (A2228, 1:5000; Sigma); rabbit anti-Tubulin (sc-9104, 1:5000, Santa Cruz Biotechnology) and horseradish-peroxidase-conjugated goat anti-rabbit or sheep anti-mouse secondary antibodies (A5906, A6154, 1:2000; Sigma). For Western blot analysis, cells were recovered from 10 cm culture dishes, washed with phosphate-buffered saline (PBS), and lysed in RIPA buffer (Sigma) with protease inhibitors (P8340; Sigma) for 20 min on ice. The lysates were cleared (10 min, 15 000*g*, 4 °C) and protein extracts were analyzed using SDS–PAGE, and Western blotting using 5% milk powder with 0.1% Tween 20 in PBS as a blocking solution.

**Immunofluorescence microscopy**

Cells were grown on glass coverslips in 6-well cluster plates to 80% confluence. The cells on coverslips were washed briefly with PBS, fixed in 2% paraformaldehyde (PFA), permeabilized with 0.5% Triton X-100 in PBS and blocked with 3% bovine serum albumin (BSA) in PBS. The cells were then immunolabeled with primary antibodies specific for PML (rabbit anti-PML, A301-167A; Bethyl Laboratories) and FLAG (mouse anti-FLAG M2, F3165; Sigma), washed with PBS, and incubated with Alexa-Fluor 649 donkey anti-rabbit, Alexa-Fluor 488 donkey anti-rabbit, and Alexa-Fluor 555 donkey anti-mouse (ThermoFisher Scientific) secondary antibodies. The cells were washed several times in PBS and incubated with 1 μg/mL of 4′,6-diamidino-2-phenylindole (DAPI) to visualize the nuclei. Fluorescent micrographs were captured with a HQ2 charge-coupled device (CCD) camera (Photometrics) on a custom-built Zeiss Cell Observer Microscope (Intelligent Imaging Innovations) using a 1.3 NA 40× immersion oil objective lens and LED illumination via a Spectra light engine (Lumencor). Images were processed and analyzed using Slidebook (Intelligent Imaging Innovations) and Adobe Photoshop CS5.

**DR-GFP HDR and CRISPR LMNA-HDR gene editing assays**

The extrachromosomal HDR assay was performed in NHDF and NHDF ΔPML cells, and involved co-transfection of the split-GFP reporter DR-GFP (pHPRT-DRGFP) and a vector encoding the rare endonuclease I-SceI (pCBASceI), as previously described (Pierce et al. 2001), with a co-transfection marker piRFP670-N1, which allowed data to be normalized for transfection efficiency. NHDF cells ($1\times10^6$) were transfected with 11 μg of DNA (DR-GFP reporter (4ug) and I-SceI (4ug), and 3ug of piRFP670-N1) using the Neon electroporation transfection system (1400 V; width, 20 ms; pulse #, 2). The cells were analyzed 72 h post-transfection.

For the CRISPR LMNA-HDR assay, $1 \times 10^6$ cells were transfected with the Neon electroporation transfection system using the following settings: NHDF cells (1400 V; width, 20 ms; pulse #, 2), U2OS cells (1230 V; width, 10 ms; pulse #, 4). The cells were transfected with 8 μg of total DNA in a 3:1 ratio of sgRNA/Cas9 plasmid pX330-LMNA (targeting the first exon of *LMNA*) to the *LMNA* homology donor pCR2.1-CloverLamin, as well as 1 μg of a co-transfection marker piRFP670-N1 as described in Pinder et al. (2015).

For the HR/HDR assays with PML isoform overexpression, U2OS, U2OS ΔPML, NHDF, and NHDF ΔPML cells were transfected with 8 μg of total plasmid DNA as described above, except that the amount of the two assay plasmids were reduced to accommodate 2 μg of either an empty FLAG vector (CMV-FLAG) or a plasmid encoding a single FLAG-tagged PML isoform (PML I-VI). At 72 h post-transfection, the NHDF cells were fixed and prepared for immunofluorescence microscopy as described above. The analysis for NHDF and NHDF ΔPML cells was performed by imaging random fields of view and then counting over 500 iRFP670-positive cells in each replicate to determine the mean Clover-positive/iRFP-positive cell count. The replicate means for each condition was then averaged to generate the mean used for statistical tests. U2OS cells were analyzed by flow cytometry at 72 h post-transfection as described below.

For chromosomal HDR repair assays, U2OS Chr15 HR and U2OS TAP1 HR cells were transfected with equal amounts of an empty FLAG vector (CMV-FLAG-J1) or an individual FLAG-tagged PML isoform (I-VI) expression vector, piRFP670-N1 (transfection control) and pBluescript SK (Stratagene) as carrier ± a β-Actin-SceI expression vector. All transfections were performed using the Neon transfection system (ThermoFisher Scientific). Cells were plated into separate 9-cm plates (each containing a sterile coverslip) and harvested for flow cytometry (as described below) with an aliquot removed for cell cycle analysis, and immunofluorescence analysis, 72 h post-transfection.

**Flow cytometry**

To ~~determining~~ the percentage of Clover- or GFP-positive cells, cells were trypsinized and resuspended in PBS. Cell suspensions were fixed in 2% PFA, washed in 25 nmol/L ammonium citrate and resuspended in PBS. For cell cycle analysis, the cells were trypsinized, and $1 \times 10^6$ cells were pelleted by centrifugation at room temperature. The pellets were resuspended in 0.5 mL PBS and fixed with the dropwise addition of 4.5 mL of 70% ice-cold ethanol with mild vortexing. Ethanol-fixed cell suspensions were incubated for at least 24 h at –20 °C. On the day of cell cycle analysis, the samples were pelleted by centrifugation, washed in PBS, and resuspended in PBS–propidium iodide (PI) solution (0.1% Triton X-100, 0.2 mg/mL RNaseA, 1 mg/mL PI) for 30 min at room temperature.

Flow cytometry was performed using a FACSCalibur flow cytometer (BD Biosciences), and analysis performed using Flowing Software (version 2.5.1; Cell Imaging Core, Turku Centre for Biotechnology, Finland). For DNA repair assays, the cells were first gated for intact cell population using forward-scatter versus side-scatter plots, and then gated for transfected cells based on the expression of the transfection control, iRFP670, using side-scatter compared with the iRFP670 plots. Transfected cells were then gated for GFP or Clover-positive cells on the side-scatter versus GFP/Clover plots, such that the percentage of iRFP670-transfected control cells (cells transfected with a specific PML isoform but without β-Actin-SceI or px330-lamin 5′ gRNA) that were designated as GFP/Clover positive was 1%. The mean and standard deviation from 3 independent replicates were calculated. Statistical analyses (2-tailed *t* test) were conducted using Excel 2010 (Microsoft) and Prism 6 (Graphpad) software. For cell-cycle analysis, the cells were gated for intact cell population (as above) and percentage of cells in each cell-cycle phase determined from plots of counts versus PI. Cell-cycle analysis was done in triplicate for each experimental condition in each cell line. Statistical analysis was performed as described above.

**Immuno-fluorescence in-situ hybridization (Immuno-FISH)**

FISH and 3D immuno-FISH protocols were adapted from the methods of Ching et al. (2013) and Cremer et al. (2008). The cells were seeded onto sterile frosted glass microscope slides (ThermoFisher Scientific) so that they would be at a confluency of 70%–80% the next day. The slides were rinsed twice in PBS at 37 °C and fixed in 4% PFA at room temperature. The cells were then washed

**Fig. 1.** Generation and validation of promyelocytic leukemia protein (PML) knock-out in U2OS and NHDF cells. The *PML* gene locus was disrupted in U2OS and TERT-immortalized GM05757 normal human diploid fibroblast (NHDF) cells using CRISPR/Cas9 and guide RNA targeting PML exon 1. (A) Western blotting for PML expression in wild-type (WT) and PML gene-edited (ΔPML) U2OS and NHDF cell lysates. (B) Relative PML mRNA levels in WT and ΔPML U2OS and NHDF cells as assessed by qRT-PCR; **, $p < 0.01$. (C) Immunofluoresence microscopy images of WT and ΔPML U2OS and NHDF cells immunostained for PML (green). DNA was visualized with DAPI (blue). Scale bar = 10 μm. [Colour online.]

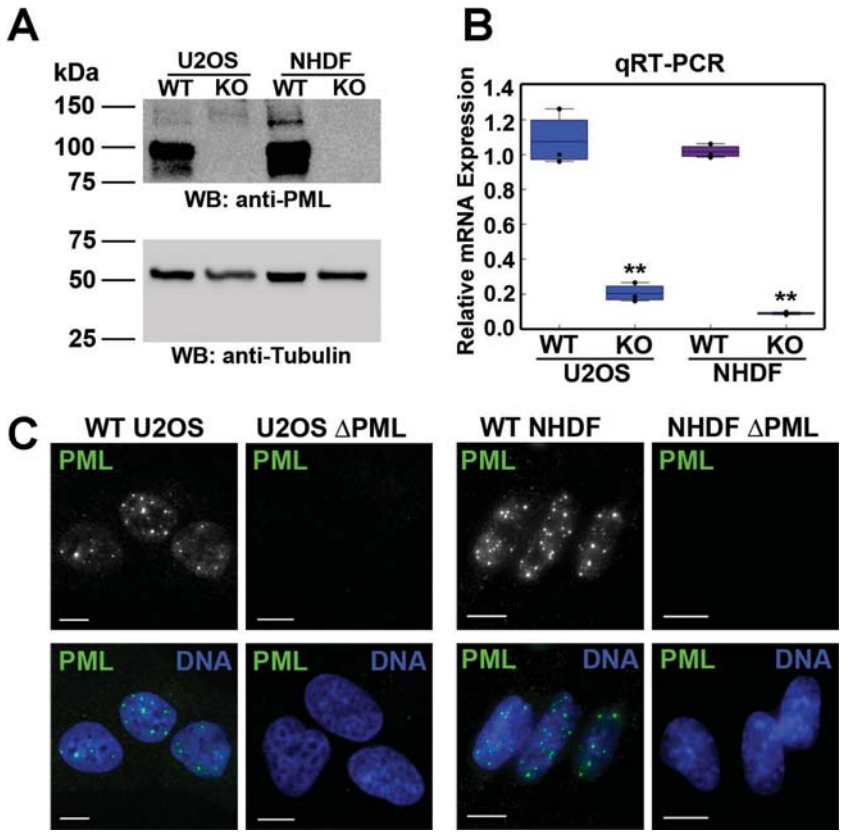


3 times in 0.01% Triton X-100, followed by a wash in 0.5% Triton X-100 and an overnight incubation in 20% glycerol, all at room temperature. The slides were then flash-frozen in liquid nitrogen, allowed to thaw completely, and then immersed back into 20% glycerol; this was repeated 4 times. The cells were subsequently washed in PBS, incubated in 0.1 mol/L HCl, washed twice in 2× SSC and incubated overnight at room temperature in 50% formamide–SSC. Spectrum Orange labeled probe generated against a pFlexible-LacO-pBLR5 (pFlex) (Supplementary data, Fig. S3[1]) or BACs containing the *Chr15*, *TAP1*, and *BCL2* loci (BAC reference: RP11105M14, RP111A19, and RP11160M23, respectively; Sick Kids Centre for Applied Genomics, Toronto, Ontario, Canada) were mixed in a 2:1 ratio with human Cot1 DNA (ThermoFisher Scientific) in pre-hybridization buffer [50% formamide, 10% dextran sulfate, 50 mmol/L sodium phosphate, (pH 7.0) in 2× SSC], denatured for 3 min at 75 °C, and hybridized with cells at 37 °C for 3 days. Following hybridization, the slides were washed 3 times in 2× SSC at 37 °C, and 3 times in 0.1× SSC at 65 °C. The cells were then rinsed briefly in SSC–Tween (4× SSC – 0.2% Tween 20) and blocked in 4% BSA in SSC–Tween at 37 °C. The cells were subsequently incubated with rabbit-anti-PML primary antibody (Bethyl) in 1% BSA SSC–Tween, washed 3 times in SSC–Tween and then incubated with Alexa Fluor 488 donkey anti-rabbit secondary antibody (ThermoFisher Scientific) in 1% BSA SSC–Tween, all at 37 °C. The cells were then washed again 3 times in SSC–Tween and incubated with DAPI at a final concentration of 1 μg/mL to visualize the nuclei. Fluorescent images were captured on a Zeiss Cell Observer Microscope (Intelligent Imaging Innovations; as described above) using a 1.4 NA 63× immersion oil objective lens and processed using Slidebook (Intelligent Imaging Innovations) and Adobe Photoshop CS5. The image stacks were exported to Imaris 7.1 (Bitplane) software, where quantification of distances between PML NBs and the Chr15, TAP1, and BCL2 FISH probes were determined. The 3D positions of the nuclei were first defined using the DAPI fluorescence signal, while the 3D position of PML NBs in the nuclei were defined using the Alexa-Fluor 488 signal from the anti-PML immunostaining and the 3D positions of the *Chr15*/*TAP1*/*BCL2* locus defined using signal from the Spectrum Orange labeled probes. The distances between the centers of the defined FISH probe objects and closest PML body in each defined nucleus were calculated and exported to Excel for analysis. Fifty nuclei were analyzed for *TAP1*, *BCL2*, and *Chr15*. The average closest distance between a PML nuclear body and the FISH signal was calculated for each probe.

### Statistical analyses and graphing

A 2-tailed Student *t* test was used for pair-wise statistical analyses, and one-way ANOVA was used for multiple comparisons, assuming a Gaussian distribution, using Prism 7.03 (GraphPad). Graphs were generated with Excel, Prism 7.03, and the PlotsOfData web application (https://huygens.science.uva.nl/PlotsOfData/) (Postma and Goedhart 2019).

## Results

### Homologous recombination and homology-directed repair is decreased in PML-knock-out cells

Although PML NBs respond to genotoxic stress by forming microbodies in an ATM-dependent manner, following induction of DNA breaks (Dellaire et al. 2006*b*; Kepkay et al. 2011), evidence for their role in the process of DNA repair has largely been inferred by

**Fig. 2.** Loss of promyelocytic leukemia protein (PML) inhibits extrachromosomal homology-directed repair (HDR) but not chromatin-associated HDR in NHDF cells. (A) Cartoon illustrating the extrachromosomal direct repeats – green fluorescent protein (DR-GFP) assay. Cleavage of the reporter with I-SceI nuclease results in GFP expression when the DNA double-strand break is repaired by homologous recombination (HR). (B) Representative images of wild-type (WT) NHDF cells transfected with the DR-GFP assay with and without I-SceI as indicated. iRFP670 expression indicates transfected cells and GFP expression indicates cells undergoing successful HDR events (arrows). DNA was visualized with DAPI (blue). (C) Vertical scatter plot of DR-GFP assay results in NHDF and NHDF ΔPML cells showing the mean ± SD ($n = 3$). Significance was determined using a 2-way Student $t$ test; *, $p < 0.05$. (D) Cartoon illustrating the chromatin-associated Clover-LMNA assay. Cleavage of the *LMNA* gene using Cas9 and LMNA-targeting gRNA results in HDR using a co-transfected donor template that places the coding sequence for the Clover fluorescent protein in-frame with exon1 of LMNA, resulting in nuclei with fluorescent nuclear lamina (fluorescent micrograph). (E) Representative images of the NHDF and NHDF ΔPML cells transfected with the Clover-LMNA assay. iRFP670 expression indicates transfected cells, and Clover expression indicates cells undergoing successful HDR events (arrows). DNA was visualized with DAPI (blue). Scale bar = 20 μm. [Colour online.]

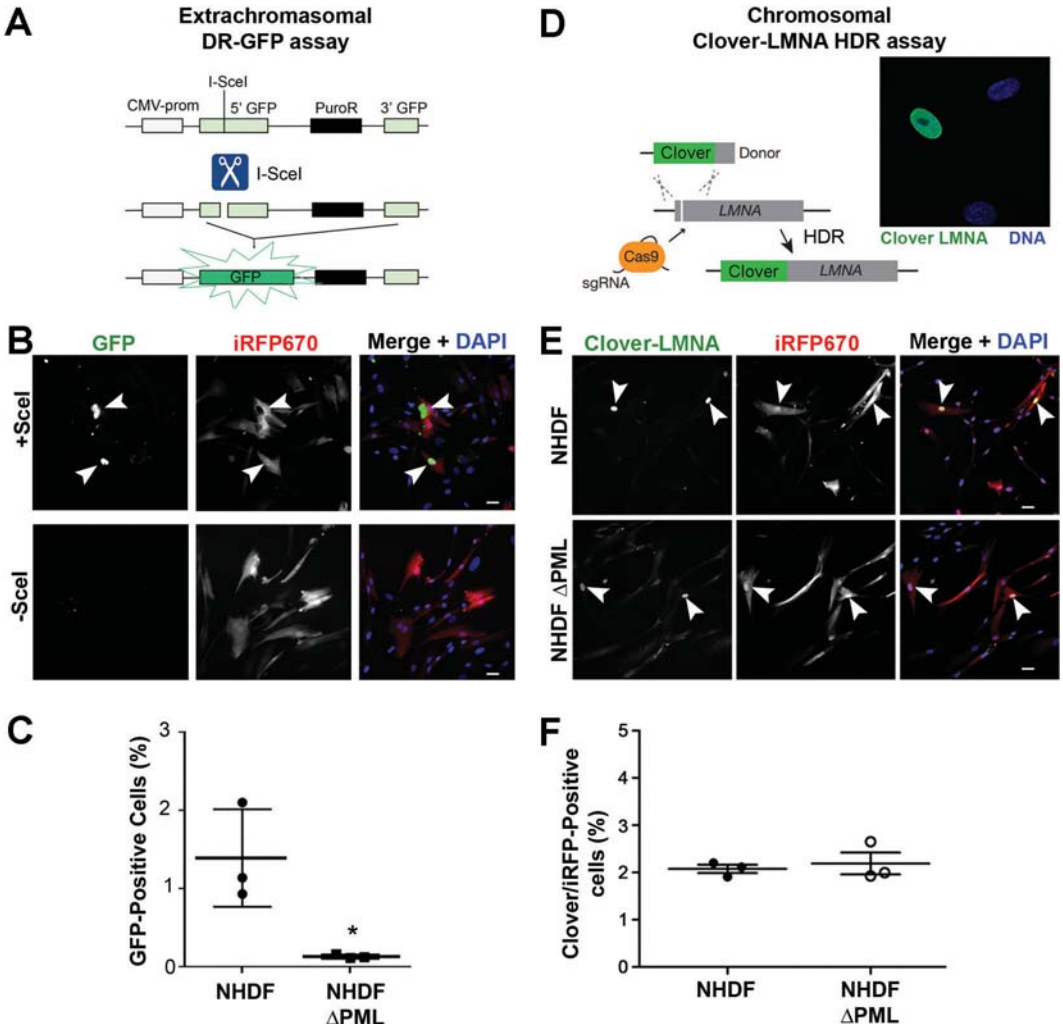


their association with DNA repair factors and their juxtaposition to "repair foci" containing damaged chromatin (Dellaire and Bazett-Jones 2004; Dellaire et al. 2009; Chang et al. 2018). More recently, evidence has emerged supporting a possible role for PML NBs in DNA DSB repair by homologous recombination (HR) (Boichuk et al. 2011; Yeung et al. 2012; Munch et al. 2014); however, the role of the PML protein isoforms and PML NB positioning in HDR has not been well studied, nor their impact on genome editing. To study the effect of PML (and PML NBs) on HR, CRISPR/Cas9-mediated genome editing was used to disrupt the *PML* gene in the TERT-immortalized normal human fibroblast cell line GM05757 (NHDF) (Kepkay et al. 2011) and in human osteosarcoma U2OS cells, creating PML knock-out (ΔPML) cell lines that do not express PML or form PML NBs (Fig. 1; Supplementary data, Figs. S1–S3[1]). Rates of HDR were then compared in wild-type (WT) and ΔPML NHDF cells using the DR-GFP extrachromosomal assay, as originally described by Pierce et al. (1999, 2001), that employs the rare endonuclease I-SceI to induce a break in a split GFP reporter gene that only produces green fluorescence when the break is repaired by HDR. Consistent with previous studies using a similar split-puromycin resistance gene HDR reporter system (Yeung et al. 2012), we observed a significant inhibition of extrachromosomal DNA repair by HDR using this system in NHDF cells (Figs. 2A–2C).

Based on the observations of reduced HDR in the NHDF ΔPML cells using an extrachromosal reporter, and given the importance of HR pathways in CRISPR-based genome editing, we decided to examine the impact of PML loss on CRISPR-mediated gene editing by HDR in WT and ΔPML NHDF cells using a gene knock-in strategy (Clover-LMNA assay) we developed for measuring HDR efficiency (Pinder et al. 2015). Briefly, cells were co-transfected with an HDR donor vector carrying the Clover gene, along with a vector expressing Cas9/gRNA targeting the second codon of the LMNA

**Fig. 3.** Loss of promyelocytic leukemia protein (PML) inhibits chromatin-associated homology directed repair (HDR) in U2OS cells. (A) Representative image of the Clover-LMNA HDR assay in U2OS cells showing Clover-lamin in green. DNA is visualized with DAPI (blue). Scale bar = 10 μm. (B) FACS analysis (top panels) of the Clover-LMNA HDR assay in wild-type U2OS and U2OS ΔPML cells. The cells were transfected with iRFP as a transfection control, and either the clover donor plasmid only or the donor plasmid with the Cas9/sgRNA vector ("clover donor + sgRNA"). The percentage of iRFP and Clover-positive cells indicates the degree of successful HDR events, which was determined for $n = 3$ independent experiments and is presented in the vertical scatter plot as the mean ± SD. Significance was determined using a 2-way Student $t$ test; *, $p < 0.05$. [Colour online.]

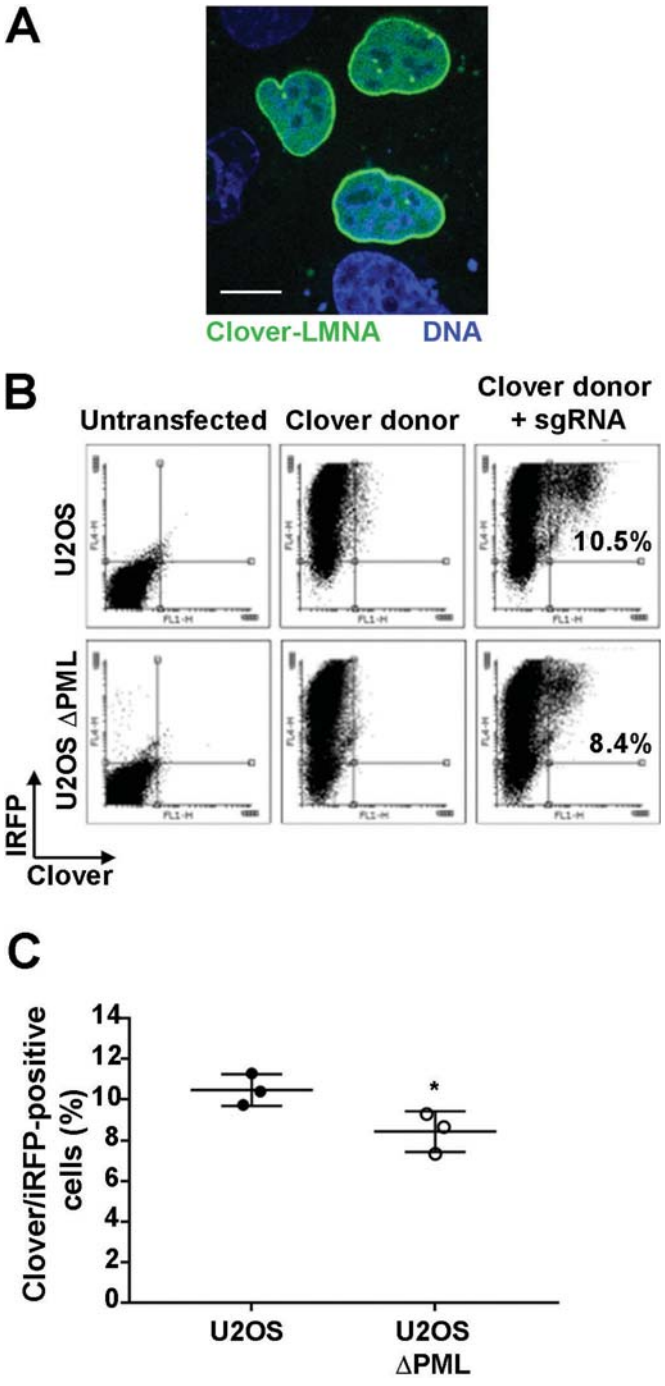


**Fig. 4.** Comparison of cell-cycle profiles of wild-type (WT) and promyelocytic leukemia protein knock-out (ΔPML) U2OS and NHDF cells. Cell-cycle analysis of WT U2OS and ΔPML cells (A) or WT NHDF and ΔPML cells (B) using propidium-iodide staining and flow cytometry. Data were derived from counting at least 10 000 events per experiment, with $n = 4$ (A, U2OS) or $n = 3$ (B, NHDF) replicates ± SD; ns, non-significant based on 2-way Student $t$ tests comparing the G1, S, or G2/M phases between WT and ΔPML cells.

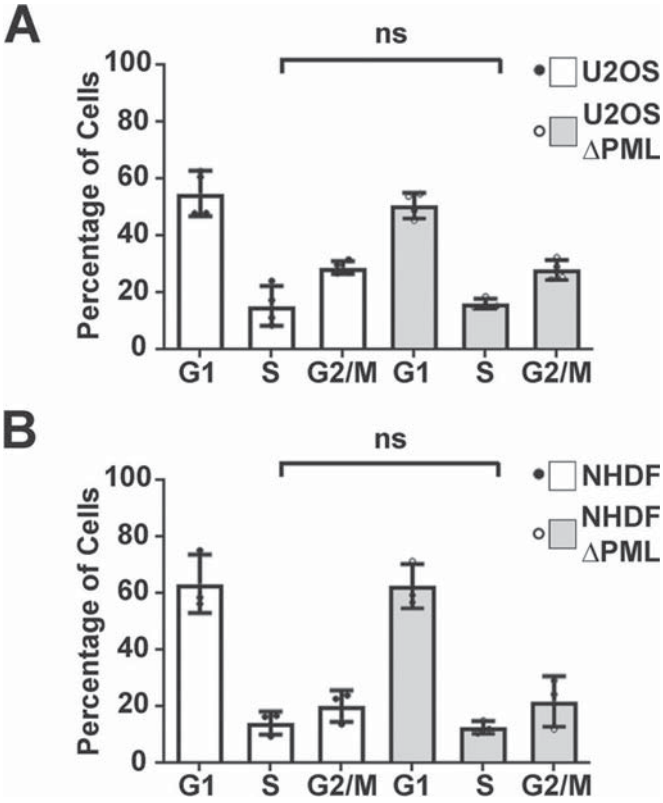


gene. Productive incorporation of Clover by CRISPR/Cas9-mediated HDR results in cells expressing fluorescent lamin A/C and thus a green nuclear lamina (Fig. 2D). To control for transfection efficiency, an expression vector for the far-red fluorescent protein, iRFP670, was co-transfected with Cas9/sgRNA and HDR donor. The cells were then analyzed by immunofluorescence microscopy to determine the percentage of transfected cells (far-red) that were Clover positive (green) and had therefore undergone CRISPR/Cas9-mediated HDR (Figs. 2E and 2F). We found that PML loss in the NHDF cells did not significantly affect chromatin-associated Cas9-mediated HDR (Fig. 2F) unlike the extrachromosomal DR-GFP assay (Fig. 2C). We also conducted the Clover-LMNA HDR assay in the U2OS and U2OS ΔPML cells to test whether PML loss might affect HDR in another cell line. Similar to the NHDF cells, expression of the Clover-LMNA assay plasmids in U2OS cells resulted in successful HDR and the appearance of Clover-tagged nuclear lamina (Fig. 3A). The transfection efficiencies in U2OS cells were substantially higher than in the difficult to transfect NHDF cells, so we could analyze these cells by fluorescence-activated cell sorting (Fig. 3B). In U2OS cells, loss of PML resulted in the percentage of iRFP670 expressing transfected cells expressing Clover-LMNA was significantly lower in ΔPML cells relative to WT U2OS. Taken together, our results indicate that PML loss can negatively impact homologous recombination in both I-SceI-based extrachromosomal HDR assays and CRISPR-mediated HDR assays, but the impact was more robust in U2OS cells. These results are also consistent with other reports (Yeung et al. 2012). However, the contrast in our results between U2OS and NHDF cells using the

**Fig. 5.** Overexpression of the promyelocytic leukemia protein (PML) isoform leads to a decrease in homology-directed repair (HDR) in wild-type (WT) and PML knock-out (ΔPML) U2OS cells. Individual FLAG-tagged PML isoforms (PMLI to PMLVI) were expressed in WT U2OS (A) or U2OS ΔPML (B) cells by transfection. The transfected cells were fixed and immunostained for anti-PML (red) and anti-FLAG (yellow), and DNA was visualized with DAPI. (C) WT U2OS and ΔPML cells were co-transfected with the Clover-lamin CRISPR donor plasmid and an empty FLAG vector, or an individual FLAG-tagged PML-isoform expression vector, either with or without Cas9/gRNA. The cells were also transfected with an iRFP expression vector as a transfection control. Shown are representative iRFP versus Clover plots and the mean percentage of Clover-positive cells from 3 independent experiments (±SD) counting at least 50 000 events per experiment. The data are normalized to cells expressing Clover-lamin CRISPR donor and specific PML isoforms without Cas9/gRNA. (D) The percentage of iRFP- and Clover-positive cells indicates the degree of successful HDR events, which was determined for $n = 3$ independent experiments and is presented in the grouped bar plot as the mean ± SD. Significant differences between the WT and U2OS ΔPML cells (with or without PML isoform expression) were determined using the 2-tailed Student $t$ test, and a 1-way ANOVA test was used for multiple comparisons of empty vector WT (or U2OS ΔPML) cells versus PML isoform transfected WT (or U2OS ΔPML) cells; *, $p < 0.05$; **, $p < 0.01$. Scale bar = 10 μm. [Colour online.]

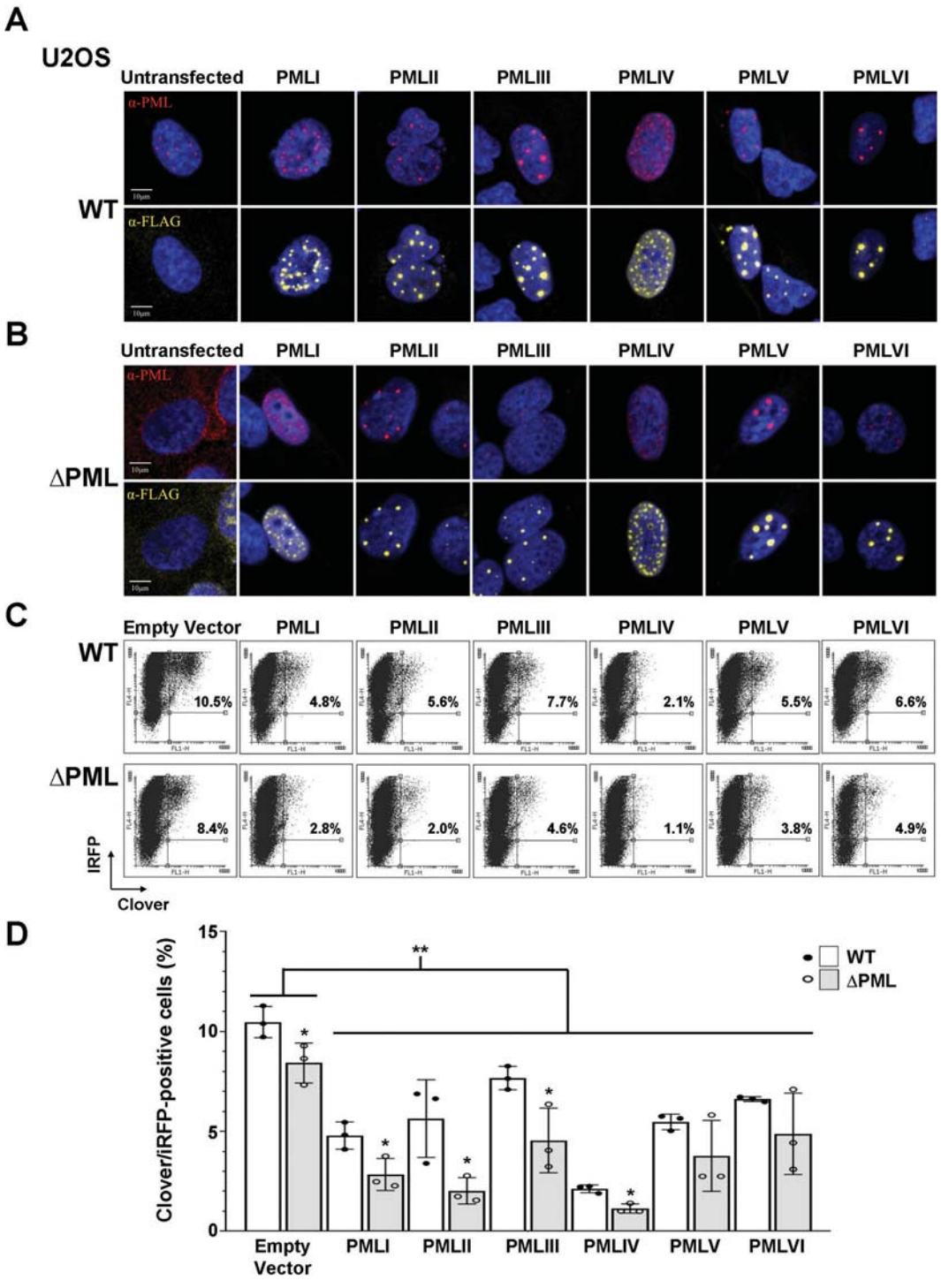

Clover-LMNA HDR assay suggests that the role of PML in supporting HDR may be cell line and (or) chromatin dependent. DNA DSB repair by HDR is cell-cycle dependent, occurring primarily in S or G2 phases (Mao et al. 2008). Therefore, to determine whether the difference in HDR repair rates observed between these two cell lines was due to differences in cell-cycle distribution, the cell-cycle profile of each cell line was determined by PI staining and flow cytometry (Fig. 4). Importantly, there was no significant reduction in cells in S-phase or G2/M between WT and ΔPML U2OS or NHDF cells. Therefore, these data indicate that loss of PML expression does not impact HDR capacity by reducing cells in S or G2-phase of the cell cycle.

### PML overexpression is inhibitory to HDR in an isoform-specific manner

Next we sought to determine the effects of PML overexpression on HDR efficiency by overexpressing PML in WT and ΔPML U2OS cells. Since it is known that individual PML protein isoforms may differentially affect cellular processes, including cell fate decisions following DNA damage (Bernardi and Pandolfi 2007), we decided to express each of the 6 nuclear isoforms of PML (PMLI to VI) in both WT and ΔPML U2OS cells (Figs. 4A–4B). To determine the effects of PML isoform overexpression on rates of CRISPR/Cas9-mediated HDR, U2OS and ΔPML cells were transiently co-transfected with the Clover-*LMNA* HDR donor plasmid, and an individual FLAG-tagged PML isoform expression vector (or empty control vector), either with or without the Cas9/gRNA expression vector targeting the *LMNA* gene. Again, iRFP670 served as a transfection control. As previously reported, PML isoform overexpression resulted in changes in PML body size and number that are isoform specific (Beech et al. 2005; Condemine et al. 2006; Weidtkamp-Peters et al. 2008) (Figs. 5A–5B). Additionally, in ΔPML U2OS cells, overexpression of individual PML isoforms is sufficient to cause de novo nuclear body formation (Ishov et al. 1999) (Fig. 5B). The cells were then analyzed by flow cytometry to determine the percentage of transfected cells that were Clover-positive, and thus the levels of HDR following individual PML-isoform overexpression (Figs. 5C–5D). The levels of Clover fluorescence were normalized to those of cells transfected without the Cas9/gRNA vector. In both U2OS and ΔPML cells, PML isoform overexpression resulted in an overall reduction in HDR to varying degrees. The most notable effect on HDR was observed upon overexpression of PMLI, II, and IV.

Again, to account for possible confounding issues due to cell effects of over-expressing the various PML isoforms, we conducted cell-cycle analysis by flow cytometry (Supplementary data, Fig. S9[1]). Although transfection alone could cause a slight increase the number of cells in G2/M, and a moderate but significant increase in cells in S phase (and decrease in G1) compared with untransfected cells, we found that the cell cycle distribution was relatively unchanged between the empty vector control transfected U2OS and ΔPML cells and those transfected with the various PML isoforms. Thus, these effects on HDR were not due to alterations in cell cycle caused by PML isoform overexpression.

Because the most pronounced effects on HDR in U2OS cells were found with expression of PMLI and PMLIV, we repeated these overexpression experiments in NHDF cells using these two PML isoforms and the Clover-LMNA HDR assay (Fig. 6A). Although there was no difference in HDR rates between the NHDF and NHDF ΔPML cells when transfected with a control plasmid or a plasmid encoding PMLI, we did observe a significant decrease in HDR in both cell lines when PMLIV was expressed (Fig. 6B). Further, the inhibitory effects on HDR were more pronounced in the ΔPML NHDF cells by comparison with the parental NHDF cells, where endogenous levels of other PML isoforms are present (Fig. 6B). Overall, these data indicate that the contribution of PML and PML NBs to HDR efficiency is likely context-dependent, with the cell type, PML isoform expression, and nuclear body compo-

**Fig. 6.** Overexpression of promyelocytic leukemia protein (PML) isoform IV leads to a decrease in homology-directed repair (HDR) in wild-type (WT) and PML knock-out (ΔPML) NHDF cells. (A and B) WT NHDF (A) and NHDF ΔPML (B) cells were co-transfected with the Clover-lamin CRISPR donor plasmid and an empty FLAG vector or an individual FLAG-tagged PML-isoform expression vector (PMLI or PMLIV) and Cas9/gRNA. The cells were also transfected with an iRFP expression vector as a transfection control. The cells were fixed and immunostained for anti-FLAG (red). DNA was visualized with DAPI (blue). The transfected cells were identified by iRFP670 expression, and successful HDR events were identified by clover-tagged nuclear lamina (green). Arrows identify specific transfected cells for assessment of clover-lamin and FLAG expression status across panels for the same experimental condition. (C) The percentage of iRFP- and Clover-positive cells indicates the degree of successful HDR events, which was determined for $n = 3$ independent experiments and is presented in the grouped bar plot as the mean ± SD. Significance between WT and NHDF ΔPML cells (with or without PML isoform expression) was determined using the 2-tailed Student $t$ test, and a 1-way ANOVA test was used for multiple comparisons of empty vector WT (or NHDF ΔPML) cells versus PML isoform transfected WT (or NHDF ΔPML) cells; *, $p < 0.05$. Scale bar = 20 μm. [Colour online.]

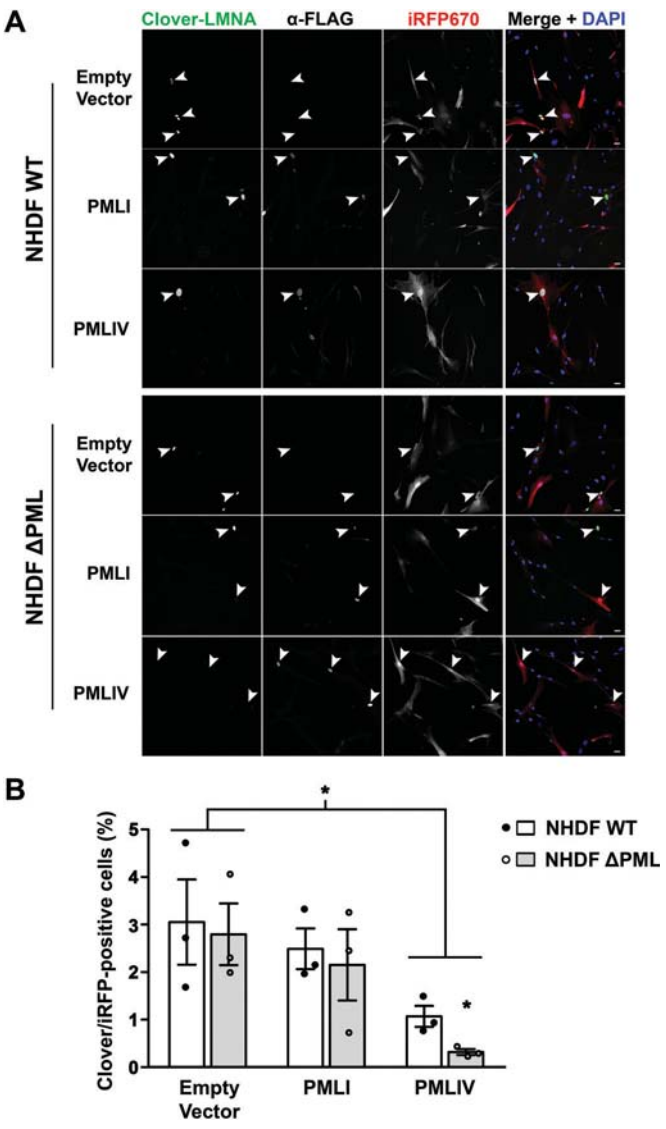

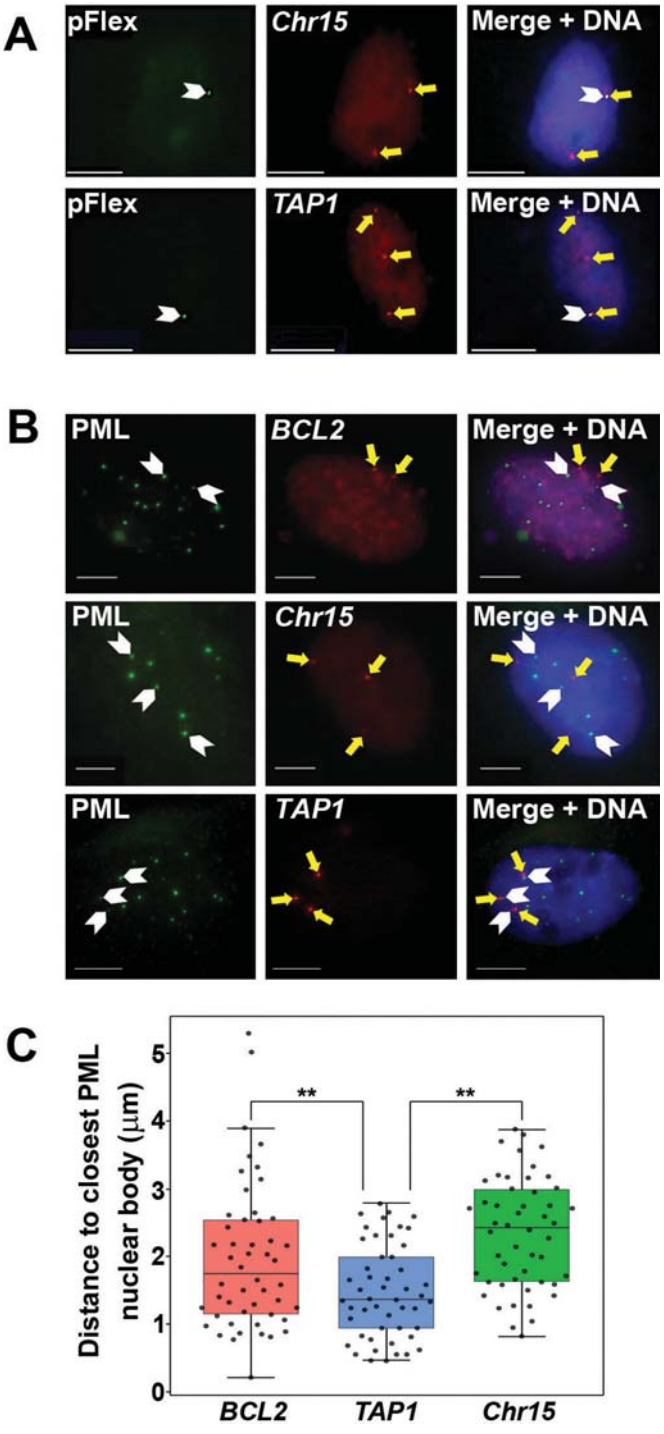


**Fig. 7.** *TAP1*, but not *BCL2* or *Chr15* genomic loci are associated with promyelocytic leukemia protein (PML) nuclear bodies (NBs). (A) Single-Z confocal FISH images of the pFlexible-LacO-pBLR5 (pFlex) construct contained at the CRISPR/Cas9-targeted *Chr15* or *TAP1* locus of U2OS cells. The DIG-labeled pFlex probe was directed against the 128x LacO array contained within the pFlex sequence, and was detected using an anti-DIG antibody (green) and is indicated with white arrows. The *Chr15* and *TAP1* loci were detected using BAC DNA probes (red) specific to each locus, and are indicated with yellow arrows. The nuclei were visualized with DAPI (blue). (B) The distances between PML NBs and the BCL2, Chr15, and TAP1 FISH probes were measured from 3D immuno-FISH image stacks. The 3D positions of the nuclei were defined using DAPI fluorescent signal, while the 3D positions of PML NBs in the nuclei were defined using signal from PML immunostaining, and 3D positions of the *BCL2*/*Chr15*/*TAP1* were loci defined using signal from Spectrum Orange-labeled probes. The distance between the centers of the defined FISH probe objects and closest PML body (depicted by white and yellow arrows respectively) in each defined nucleus was calculated. (C) At least 50 nuclei were analyzed for each probe and the average closest distance between a PML nuclear body and FISH signal was calculated for each probe. Significant differences were determined using a 2-way Student *t* test; **, $p < 0.01$. Scale bar = 10 μm. [Colour online.]

sition being pertinent variables. Given that >100 proteins localize to the PML NB, it is also likely that changes in PML isoform expression could alter the levels of these factors, further contributing to the regulation of chromatin transactions including DNA transcription, replication, and repair (Ching et al. 2005; Dellaire and Bazett-Jones 2007).

### HDR is reduced at a genomic locus significantly associated with PML nuclear bodies

We next wanted to further explore how the genomic context of a DNA break might affect how PML contributes to HDR. PML NBs have been shown to associate with certain genomic loci (e.g., *TAP1*) but not others (e.g., *BCL2*) to regulate gene expression (Shiels et al. 2001; Ching et al. 2013; Salsman et al. 2017). We hypothesized that this proximity could also influence the efficiency of DNA repair. Therefore, to determine how the proximity of a PML NB to damaged chromatin could contribute to the efficiency of HR-mediated DNA DSB repair, we used CRISPR/Cas9 gene editing to generate cell lines containing the DR-GFP HDR reporter "knocked-into" cell lines in which a sequential targeting vector system based on pFlexible (van der Weyden et al. 2005) and containing a 128 copies of the Lac Operator (pFlexible-LacO-pBLR5, Supplementary data, Fig. S4[1]) were integrated within either exon 1 of the *TAP1* gene or an intergenic region of human chromosome 15 (GRCh37.p.13 primary assembly chr15:74696007-74698086, referred to as *Chr15*) using CRISPR/Cas9 (details in the Supplementary data, Figs. S4–S7[1] and Supplemental Methods).

The *TAP1* gene is located within the MHC class II gene-cluster region, which has been found to be significantly associated with PML NBs. Genomic PCR amplification (Supplementary data, Fig. S8[1]) and 3-dimensional in situ hybridization (3D-FISH) (Cremer et al. 2008) using BAC probes directed against the individual *Chr15* and *TAP1* loci enabled confirmation of correct targeted insertion of the pFlexible-LacO-pBLR5 (pFlex probe) at the target sites (Fig. 7A). Exact colocalization of the pFlexible-LacO-pBLR5 construct was observed with the *Chr15* locus in U2OS Chr15 pFlex cells and the *TAP1* locus in U2OS TAP1 pFlex cells. U2OS cells are aneuploid and contain 3 copies of chromosomes 6 and 15; however, FISH revealed that the pFlexible-LacO-pBLR5 construct was integrated at only one of the 3 alleles in each cell line (Fig. 7A). The DR-GFP reporter system was inserted into the pFlex construct using Crispr/Cas9-mediated gene editing (details in the Supplementary data, Figs. S4–S7[1] and Supplemental Methods), and correct integration of the DR-GFP reporter was confirmed through genomic PCR (Supplementary data, Fig. S8[1]).

In addition, 3D-immuno-FISH was used to determine the respective distance between PML NBs (detected by indirect immunofluorescence) and BAC probes directed against either the *Chr15* or *TAP1* locus in U2OS cells. It was confirmed that the *TAP1* locus is significantly associated with PML NBs when compared with *BCL2*, a locus known to not associate with PML NBs (Ching et al. 2013). Similar to *BCL2*, the *Chr15* locus was found to not associate with PML NBs (Figs. 7B and 7C). Thus, by choosing these two genomic regions, a comparison of HDR could be made between chromatin in close proximity to PML NBs (the *TAP1* locus) or unassociated with these bodies (the *Chr15* locus).

**Fig. 8.** Comparison of homology-directed repair (HDR) rates in U2OS Chr15 and TAP1 homologous recombination (HR) cell lines. (A) Immunofluoresence microscopy images of FLAG-tagged promyelocytic leukemia protein (PML) isoform expression in the U2OS Chr15 and TAP1 HR cell lines showing total PML (anti-PML immunostain, red) and PML isoform expression (anti-FLAG, yellow). DNA was visualized with DAPI (blue). (B) U2OS Chr15 HR and U2OS TAP1 HR cells were transfected with plasmids encoding FLAG-tagged PML isoforms and an iRFP expression vector with or without an I-SceI endonuclease expression vector. Seventy-two hours post-transfection, the cells were fixed and analyzed by flow cytometry. The percentage of iRFP- and GFP-positive cells indicates the degree of successful HDR events, which was determined for 3 independent experiments and is presented in the candle plot as the mean ± SE. The 2-tailed Student *t* test was used to determine the significance of the difference in percentage of transfected Chr15 versus TAP1 HR cells, and a 1-way ANOVA test was used for multiple comparisons of empty vector Chr15 HR cells versus PML isoform transfected Chr15 HR cells. Note, only PMLI-transfected TAP1 HR cells exhibited significantly different HDR efficiency compared with empty vector transfected TAP1 HR cells; *, $p < 0.05$; **, $p < 0.01$; ***, $p < 0.001$. Scale bar = 10 μm. [Colour online.]

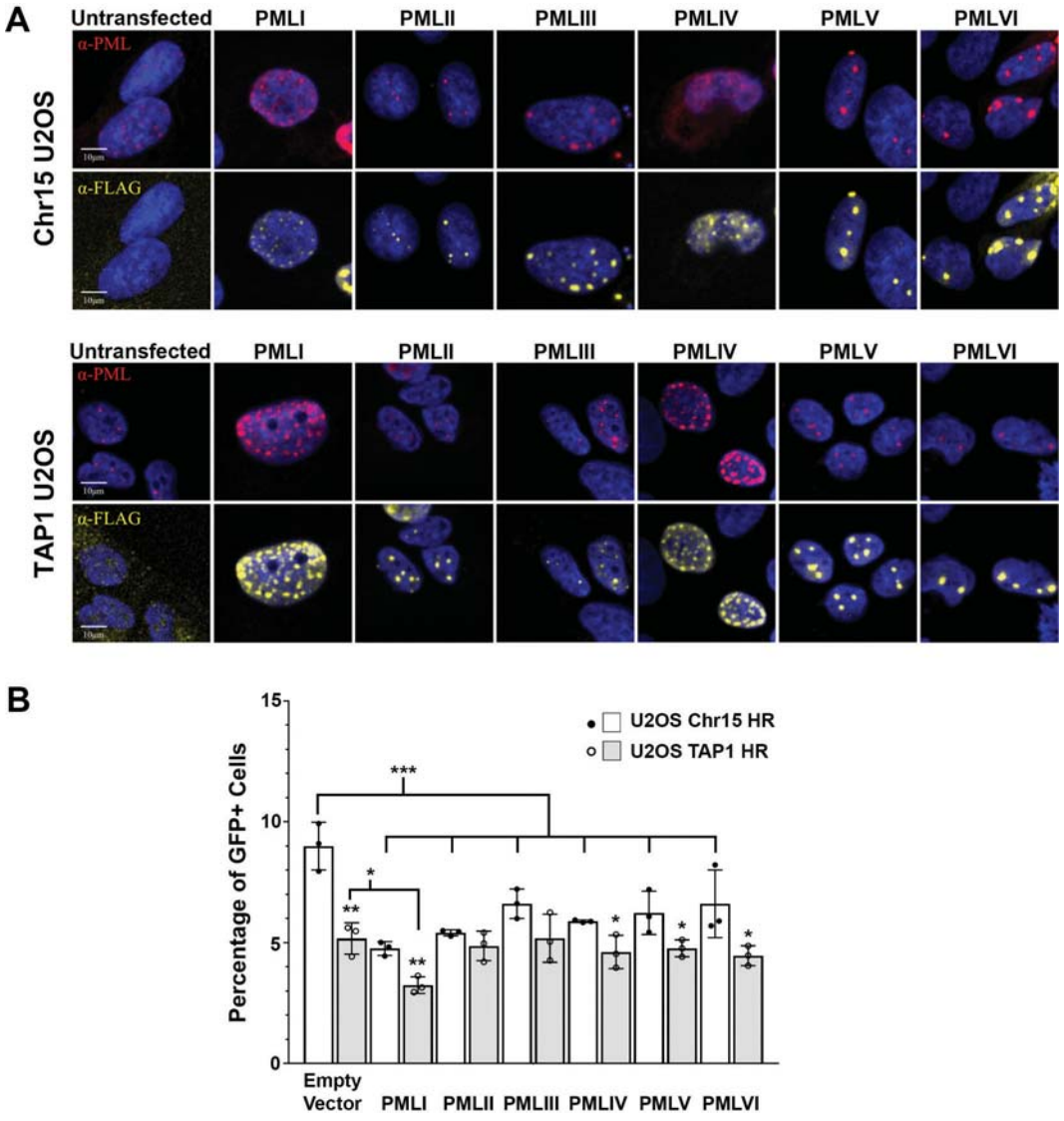


U2OS Chr15 HR and U2OS TAP1 HR cells were transiently transfected with an I-SceI expression vector to induce a DSB in the DR-GFP HDR reporter DNA, along with a vector expressing iRFP as a transfection control. The cells were then analyzed by flow cytometry to determine the percentage of transfected cells (iRFP+) that were GFP positive, and had therefore undergone a DNA repair event by HR (Fig. 8). The percentage of transfected cells expressing GFP was significantly higher in cells in which the DR-GFP HDR reporter was integrated at the *Chr15* locus (approximately 9% of transfected cells) relative to *TAP1* (5% of transfected cells) ($p < 0.01$) (Fig. 8). To determine whether the difference in HDR repair rates observed between these two cell lines was due to differences in cell-cycle distribution, the cell-cycle profiles of each cell line were analyzed by flow cytometry (Supplementary data, Fig. S10[1]). No significant differences in cell-cycle profiles were observed between the two cell lines, indicating that the difference in HDR can likely be attributed to the difference in nuclear positioning of the reporter DNA.

Finally, we sought to determine how PML isoform overexpression might affect the repair of chromosomal DNA breaks by HDR at loci adjacent to or spatially separate from PML NBs in U2OS cells. To accomplish this, we transfected U2OS Chr15 HR and TAP1 HDR reporter cells with an empty FLAG vector or an individual expression vectors encoding various FLAG-tagged PML-isoforms with or without a vector expressing I-SceI; which is required to initiate a DNA break in the chromosome-integrated DR-GFP HDR reporter in these cells. Similar to the results of the Clover-lamin HDR assay, the chromosomal HDR assay in U2OS Chr15 HR cells

indicated that PML isoform overexpression significantly reduced HDR at the *Chr15* locus (Fig. 8), which was not due to alterations in cell-cycle profiles (Supplementary data, Fig. S9[1]). However, in U2OS TAP1 HR cells, HDR levels did not significantly differ upon PML isoform overexpression, with the exception of PMLI (Fig. 8). Thus, taken together, our studies indicate that loss of PML and overexpression of PML isoforms can inhibit HDR, and that the position of the DNA break relative to a PML NB can impact the efficiency of homologous recombination.

## Discussion

PML NBs and, to a lesser extent, the PML protein itself have long been implicated as playing a role in the cellular response to DNA damage. Several DDR factors are known to associate constitutively with PML NBs, while others associate only transiently, being specifically recruited to or released from bodies after damage (Dellaire and Bazett-Jones 2004). These include DNA damage sensing and transducing factors such as the MRN complex, ATM, ATR, TOPBP1, and CHK2, and multiple proteins involved in HR (RAD51, BLM, RPA, WRN, BRCA1) (Chang et al. 2018; Dellaire and Bazett-Jones 2004). The PML protein itself is a target of phosphorylation by CHK2 (Yang et al. 2002), and ATM- and ATR-mediated signaling events regulate nuclear body integrity in response to DNA damage (Dellaire et al. 2006*b*). One of the many theorized functions for PML NBs is as a cellular storage depot (Negorev and Maul 2001). In the context of DNA repair, bodies may play a temporally important role, sequestering or releasing factors as necessary following damage (Dellaire and Bazett-Jones 2004, 2007). Owing to the large number of repair factors associated with PML bodies, it is thought that DNA breaks occurring close to bodies may be repaired with increased efficiency, as PML NBs may be providing a favorable environment for DNA repair. However, repair within PML body-associated DNA has not been investigated. Additionally, while PML has been implicated in DNA repair, as described above, and disruption of PML NBs results in impaired DNA repair (di Masi et al. 2016), the exact role of the PML protein and PML NBs on DNA repair is not fully understood. Previous studies have focused on primarily linking PML/PML NBs specifically to HR, with conflicting reports as to the exact involvement of PML. Boichuk et al. 2011 demonstrated a potential role of PML in early stages of HR. Knock-down of PML was found to cause a decrease in HR, with subsequent loss of RPA, RAD51, and BRCA1 in DNA repair foci, suggesting that PML is required for DNA break processing (Boichuk et al. 2011). However, Yeung et al. 2012 also found PML depletion to be inhibitory to HDR, yet found no effect on RAD51 foci formation and demonstrated a normal induction of γ-H2AX, indicating PML involvement at later steps in the HR pathway (Yeung et al. 2012). Furthermore, Yeung et al., also demonstrated a 1.5-fold increase in DNA integration in PML knock-down by non-homologous end-joining (NHEJ) (Yeung et al. 2012), which might be expected for cells with impaired HR repair that have switched to NHEJ for the repair of DNA breaks. Also consistent with impaired DNA repair by HR, PML loss has been shown to enhance sensitivity to chemotherapeutics that target cells with HR-deficiency, including cisplatin and PARP-inhibitor olaparib (Vancurova et al. 2019). Finally, PML NB resident proteins such as ATRX have also been shown to play a role in HR. Specifically, ATRX knock-down in HeLa cells reduced HDR efficiency, and in U2OS cells deficient in ATRX, the ratio of short- versus long-track gene conversion and cross-over during HDR was altered; with add-back of ATRX in U2OS cells increasing long-track recombination at the expense of short-track HDR via synthesis-dependent strand annealing (SDSA) (Juhasz et al. 2018).Thus, in our experiments we have chosen to employ both ATRX proficient (GM05757) and deficient (U2OS) cells lines.

### I-SceI-induced HDR and CRISPR-based HDR are dependent on the presence of PML/PML nuclear bodies

As a baseline for comparison with previous studies examining PML loss and HDR, which were based on split-gene reporter assays (Boichuk et al. 2011; Yeung et al. 2012), we used the DR-GFP assay developed by Maria Jasin (Pierce et al. 1999, 2001). Similar to previous studies, we found that loss of PML significantly inhibited HDR using this assay in the TERT-immortalized normal human diploid fibroblast cell line GM0575 (NHDF; Fig. 1, $p < 0.03$). We also determined that gene editing by HDR was also affected upon loss of PML, by employing a CRISPR-based knock-in assay (Pinder et al. 2015). In the U2OS, but not the NHDF cell lines, PML knock-out (ΔPML) exhibited a modest but significant decrease in CRISPR-mediated HDR relative to the WT cells (Figs. 2 and 3), which is consistent with previous reports indicating that PML loss can negatively impact HR (Boichuk et al. 2011; Yeung et al. 2012). Because DNA repair by HDR is restricted to the S and G2 phases of the cell cycle, owing to the action of both cyclin-dependent kinases and the Cul3/Keap1 E3 ubiquitin ligase complex (Rothkamm et al. 2003; Huertas and Jackson 2009; Orthwein et al. 2015), thus PML loss might affect the cell cycle leading to the observed reduction in HDR efficiency. In our experiments in U2OS and NHDF cells, PML loss did not significantly affect the cell-cycle distribution (Fig. 4), and thus the differences in HDR rates seen with knock-out of PML cannot be attributed to cell-cycle changes. Given that disruption of PML NBs results in impaired DNA repair (di Masi et al. 2016), it is therefore most likely that impaired DNA repair is responsible for the reduced HR and HDR efficiency when PML expression is lost.

### Overexpression of all nuclear PML isoforms can inhibit HDR

Although the PML protein has been implicated in DNA repair (Carbone et al. 2002; Dellaire and Bazett-Jones 2004; Boichuk et al. 2011; Yeung et al. 2012; di Masi et al. 2016), the contribution of each of the individual PML isoforms has not been investigated. The effect of individually overexpressing each of the 6 nuclear PML isoforms on HDR was examined in WT and ΔPML U2OS cells by CRISPR-HDR assay (Fig. 5). Transient overexpression of PML isoforms induced formation of bodies that are altered in size and number, and an overall repression of HDR, but did not significantly affect cell-cycle progress in empty vector or PML isoform transfected cells (Supplementary data, Fig. S9[1]). However, we did see a reproducible increase in S-phase cells (and decrease in G1) that was modest but significant between untransfected and transfected cells in all of the experiments (Supplementary data, Figs. S9 and S10[1]). Yeung and colleagues also saw a modest but significant inhibition of HDR in HT1885 fibrosarcoma cells over-expressing PML isoforms IV and VI (Yeung et al. 2012); a finding we now extend with analyses of all nuclear PML isoforms in U2OS cells. The most notable decrease in this study was observed upon overexpression of PMLI, II, and IV; an effect that was consistent across wild-type and ΔPML U2OS cell lines. Further, the inhibitory effect of PMLIV expression on HDR was also observed NHDF and ΔPML NHDF cells (Fig. 6). Although beyond the scope of this study, these data raise the intriguing possibility that the unique C-terminus of each of these isoforms may differentially regulate DNA repair, possibly through as yet to be defined isoform specific protein–protein interactions.

### Association of a DNA break with PML nuclear bodies can inhibit its repair by HR

The *TAP1* locus has been previously shown to be significantly associated with PML NBs in human B-lymphocytes and fibroblast cells (Shiels et al. 2001; Ching et al. 2013). This was confirmed in this study in U2OS cells (Fig. 7). In this study we have also identified an intergenic region on chromosome 15 (*Chr15*, hg19;chr15:74696007-74698086), which was found not to be associated with

PML NBs to an even greater extent than the known negative control locus *BCL2*. (Figs. 7B and 7C). We could apply this knowledge of genomic locus and PML NB associations to test how the proximity of genomic DNA with PML NBs contributes to HDR efficiency by knocking-in the DR-GFP assay into the *TAP1* and *Chr15* loci of U2OS cells (Fig. 8). A significant decrease in HDR was observed in the TAP1-HR cells relative to the Chr15-HR cells, which was not due to differences in cell-cycle distribution between these two cell lines (Supplementary data, Fig. S10[1]). This marks the first time that DNA repair efficiency has been directly measured relative to PML NB proximity.

Given that PML loss inhibits HDR repair, and that a variety of repair factors are known to be located constitutively or transiently with PML NBs (Dellaire and Bazett-Jones 2004), this is somewhat of a surprising finding. It is interesting to note that PMLI and IV, and to a lesser extent PMLII (Fig. 5), not only decreased HR to the greatest extent but also resulted in a large increase in PML NBs. Based on the finding that HR was decreased at a locus significantly associated with PML NBs, we hypothesize that an increase in PML body number could lead to an increased likelihood of a DSB occurring in proximity to a body, and thus negatively impacting its repair. Along these lines, it is intriguing that PML isoform overexpression (with the exception of PMLI) in TAP HR cells did not result in a significant change in HDR levels (Fig. 8). This begs the question as to whether the pre-existing proximity of the DSB to PML NBs in these cells precludes additional inhibitory effects of PML overexpression on HDR. Based on the data presented here, closer association of a DNA DSB with PML NBs appears to negatively influence HDR, yet ultimately PML or PML NBs are required in at least some capacity for HR DNA repair.

An important corollary to our findings that overexpression of all PML isoforms can impact HDR, is that attempts to tether a DNA locus to a PML NB by dCas9 approaches (e.g., CRISPR-GO; Wang et al. 2018) or via Lac operator/Lac repressor interactions, as demonstrated by Soutoglou and colleagues in examining DNA repair at the nuclear lamina (Lemaitre et al. 2014), would be confounded by the impact on HDR of simply over-expressing the PML isoform used in targeting to this nuclear subcompartment. This was the main reason we opted to use CRISPR/Cas9 gene editing to insert the DR-GFP reporter into different loci, rather than to attempt tethering.

Overall, in this study, the role of PML and PML NBs in DNA repair has been investigated in multiple ways. Repair was studied in the context of PML knock-out, PML isoform overexpression, as well as DSB-PML body proximity. PML depletion was found to be inhibitory to both I-SceI-induced and CRISPR-mediated HDR, while PML isoform overexpression was also found to be overall repressive. Additionally, decreased HDR repair was observed at a DNA break located within chromatin significantly associated with PML NBs. Investigating the role of PML can be complicated. PML NBs are complex subnuclear domains that are associated with a large number of seemingly unrelated proteins, spanning a broad functional spectrum. It can be difficult to separate the activities attributed to the PML protein with those associated with PML NBs, as the formation and function of PML NBs is greatly impacted by the SUMOylation state of PML and PML NB-associated proteins, as well as when the intracellular levels of PML protein are altered through depletion or overexpression (Shen et al. 2006). Even when PML is knocked-out and then reintroduced as a single isoform, de novo PML NBs form and HDR is inhibited. Thus, one is left asking what possible role could PML NBs play in suppressing DNA repair by HR? A possible clue may come from several studies including our own indicating that following DNA damage resected ssDNA associated with replication protein A (RPA) is associated with PML NBs (Boe et al. 2006; Dellaire et al. 2006*b*; Munch et al. 2014); a precursor form of processed DNA at a DNA DSB that is required for HR repair but is prior to RAD51 filament formation (Ceccaldi et al. 2016; Ducy et al. 2019). This association of ssDNA and RPA with PML NBs suggests that under certain conditions, such as replication fork stalling or collapse following DNA damage, PML NBs might serve to sequester ssDNA to inhibit inappropriate HR during S-phase. Indeed, hydroxy urea treatment of cells, which is known to induce replication fork stalling and strongly activates HR (Bianchi et al. 1986; Lundin et al. 2002), results in a dramatic increase in ssDNA foci associated with PML NBs (Boe et al. 2006). Nonetheless, it is clear through this study and those examining the role of PML in DNA repair, that PML and PML NBs have a complex relationship with DSB repair pathways.

## Acknowledgements

This work was supported by a Discovery Grant from the Natural Science and Engineering Research Council of Canada (NSERC) to G.D. (RGPIN 05616); G.D. is a Senior Scientist of the Beatrice Hunter Cancer Research Institute (BHCRI). K.M.A. was supported by a Killam Trust Predoctoral Scholarship, and studentships from NSERC and the BHCRI, with funds provided by The Terry Fox Foundation. D.C. was supported by a Nova Scotia Graduate Scholarship, and S.M. is supported by a Canada Graduate Scholarship (NSERC), a Killam Trust Predoctoral Scholarship, and the Scotia Scholars Award from the Nova Scotia Health Research Foundation (NSHRF).

## References

Beech, S.J., Lethbridge, K.J., Killick, N., McGlincy, N., and Leppard, K.N. 2005. Isoforms of the promyelocytic leukemia protein differ in their effects on ND10 organization. Exp. Cell Res. **307**(1): 109–117. doi:10.1016/j.yexcr.2005.03.012.

Bernardi, R., and Pandolfi, P.P. 2007. Structure, dynamics and functions of promyelocytic leukaemia nuclear bodies. Nat. Rev. Mol. Cell Biol. **8**(12): 1006–1016. doi:10.1038/nrm2277.

Bianchi, V., Pontis, E., and Reichard, P. 1986. Changes of deoxyribonucleoside triphosphate pools induced by hydroxyurea and their relation to DNA synthesis. J. Biol. Chem. **261**(34): 16037–16042. PMID:3536919.

Boden, M., Dellaire, G., Burrage, K., and Bailey, T.L. 2010. A Bayesian network model of proteins' association with promyelocytic leukemia (PML) nuclear bodies. J. Comput. Biol. **17**(4): 617–630. doi:10.1089/cmb.2009.0140.

Boe, S.O., Haave, M., Jul-Larsen, A., Grudic, A., Bjerkvig, R., and Lonning, P.E. 2006. Promyelocytic leukemia nuclear bodies are predetermined processing sites for damaged DNA. J. Cell Sci. **119**(Pt. 16): 3284–3295. doi:10.1242/jcs.03068. PMID:16868026.

Boichuk, S., Hu, L., Makielski, K., Pandolfi, P.P., and Gjoerup, O.V. 2011. Functional connection between Rad51 and PML in homology-directed repair. PLoS ONE, **6**(10): e25814. doi:10.1371/journal.pone.0025814.

Boisvert, F.M., Hendzel, M.J., and Bazett-Jones, D.P. 2000. Promyelocytic leukemia (PML) nuclear bodies are protein structures that do not accumulate RNA. J. Cell Biol. **148**(2): 283–292. PMID:10648561.

Boisvert, F.M., Dery, U., Masson, J.Y., and Richard, S. 2005*a*. Arginine methylation of MRE11 by PRMT1 is required for DNA damage checkpoint control. Genes Dev. **19**(6): 671–676. doi:10.1101/gad.1279805.

Boisvert, F.M., Hendzel, M.J., Masson, J.Y., and Richard, S. 2005*b*. Methylation of MRE11 regulates its nuclear compartmentalization. Cell Cycle **4**(7): 981–989. doi:10.4161/cc.4.7.1830.

Carbone, R., Pearson, M., Minucci, S., and Pelicci, P.G. 2002. PML NBs associate with the hMre11 complex and p53 at sites of irradiation induced DNA damage. Oncogene, **21**(11): 1633–1640. doi:10.1038/sj.onc.1205227.

Ceccaldi, R., Rondinelli, B., and D'Andrea, A.D. 2016. Repair pathway choices and consequences at the double-strand break. trends. Cell Biol. **26**(1): 52–64. doi:10.1016/j.tcb.2015.07.009.

Chang, H.R., Munkhjargal, A., Kim, M.J., Park, S.Y., Jung, E., Ryu, J.H., et al. 2018. The functional roles of PML nuclear bodies in genome maintenance. Mutat. Res. **809**: 99–107. doi:10.1016/j.mrfmmm.2017.05.002.

Ching, R.W., Dellaire, G., Eskiw, C.H., and Bazett-Jones, D.P. 2005. PML bodies: a meeting place for genomic loci? J. Cell Sci. **118**(Pt. 5): 847–854. doi:10.1242/jcs.01700.

Ching, R.W., Ahmed, K., Boutros, P.C., Penn, L.Z., and Bazett-Jones, D.P. 2013. Identifying gene locus associations with promyelocytic leukemia nuclear bodies using immuno-TRAP. J. Cell Biol. **201**(2): 325–335. doi:10.1083/jcb.201211097.

Condemine, W., Takahashi, Y., Zhu, J., Puvion-Dutilleul, F., Guegan, S., Janin, A., et al. 2006. Characterization of endogenous human promyelocytic leukemia isoforms. Cancer Res. **66**(12): 6192–6198. doi:10.1158/0008-5472.CAN-05-3792.

Cong, L., Ran, F.A., Cox, D., Lin, S., Barretto, R., Habib, N., et al. 2013. Multiplex genome engineering using CRISPR/Cas systems. Science **339**(6121): 819–823. doi:10.1126/science.1231143.

Cremer, M., Grasser, F., Lanctot, C., Muller, S., Neusser, M., Zinner, R., et al. 2008.

Multicolor 3D fluorescence in situ hybridization for imaging interphase chromosomes. Methods Mol. Biol. **463**: 205–239. doi:10.1007/978-1-59745-406-3_15.

Dellaire, G., and Bazett-Jones, D.P. 2004. PML nuclear bodies: dynamic sensors of DNA damage and cellular stress. Bioessays, **26**(9): 963–977. doi:10.1002/bies.20089.

Dellaire, G., and Bazett-Jones, D.P. 2007. Beyond repair foci: subnuclear domains and the cellular response to DNA damage. Cell Cycle, **6**(15): 1864–1872. doi:10.4161/cc.6.15.4560.

Dellaire, G., Farrall, R., and Bickmore, W.A. 2003. The Nuclear Protein Database (NPD): sub-nuclear localisation and functional annotation of the nuclear proteome. Nucleic Acids Res. **31**(1): 328–330. PMID:12520015.

Dellaire, G., Ching, R.W., Dehghani, H., Ren, Y., and Bazett-Jones, D.P. 2006*a*. The number of PML nuclear bodies increases in early S phase by a fission mechanism. J. Cell Sci. **119**(Pt. 6): 1026–1033. doi:10.1242/jcs.02816.

Dellaire, G., Ching, R.W., Ahmed, K., Jalali, F., Tse, K.C., Bristow, R.G., et al. 2006*b*. Promyelocytic leukemia nuclear bodies behave as DNA damage sensors whose response to DNA double-strand breaks is regulated by NBS1 and the kinases ATM, Chk2, and ATR. J. Cell Biol. **175**(1): 55–66. doi:10.1083/jcb.200604009.

Dellaire, G., Kepkay, R., and Bazett-Jones, D.P. 2009. High resolution imaging of changes in the structure and spatial organization of chromatin, gamma-H2A.X and the MRN complex within etoposide-induced DNA repair foci. Cell Cycle, **8**(22): 3750–3769. doi:10.4161/cc.8.22.10065.

di Masi, A., Cilli, D., Berardinelli, F., Talarico, A., Pallavicini, I., Pennisi, R., et al. 2016. PML nuclear body disruption impairs DNA double-strand break sensing and repair in APL. Cell Death Dis. **7**: e2308. doi:10.1038/cddis.2016.115.

Ducy, M., Sesma-Sanz, L., Guitton-Sert, L., Lashgari, A., Gao, Y., Brahiti, N., et al. 2019. The tumor suppressor PALB2: inside out. Trends. Biochem. Sci. **44**(3): 226–240. doi:10.1016/j.tibs.2018.10.008.

Eskiw, C.H., Dellaire, G., and Bazett-Jones, D.P. 2004. Chromatin contributes to structural integrity of promyelocytic leukemia bodies through a SUMO-1-independent mechanism. J. Biol. Chem. **279**(10): 9577–9585. doi:10.1074/jbc.M312580200.

Everett, R.D., and Chelbi-Alix, M.K. 2007. PML and PML nuclear bodies: implications in antiviral defence. Biochimie, **89**(6–7): 819–830. doi:10.1016/j.biochi.2007.01.004.

Fagioli, M., Alcalay, M., Pandolfi, P.P., Venturini, L., Mencarelli, A., Simeone, A., et al. 1992. Alternative splicing of PML transcripts predicts coexpression of several carboxy-terminally different protein isoforms. Oncogene, **7**(6): 1083–1091. PMID:1594241.

Gurrieri, C., Capodieci, P., Bernardi, R., Scaglioni, P.P., Nafa, K., Rush, L.J., et al. 2004. Loss of the tumor suppressor PML in human cancers of multiple histologic origins. J. Natl. Cancer Inst. **96**(4): 269–279. PMID:14970276.

Haupt, S., Mitchell, C., Corneille, V., Shortt, J., Fox, S., Pandolfi, P.P., et al. 2013. Loss of PML cooperates with mutant p53 to drive more aggressive cancers in a gender-dependent manner. Cell Cycle, **12**(11): 1722–1731. doi:10.4161/cc.24805.

Huertas, P., and Jackson, S.P. 2009. Human CtIP mediates cell cycle control of DNA end resection and double strand break repair. J. Biol. Chem. **284**(14): 9558–9565. doi:10.1074/jbc.M808906200.

Jensen, K., Shiels, C., and Freemont, P.S. 2001. PML protein isoforms and the RBCC/TRIM motif. Oncogene, **20**(49): 7223–7233. doi:10.1038/sj.onc.1204765.

Juhasz, S., Elbakry, A., Mathes, A., and Lobrich, M. 2018. ATRX promotes DNA repair synthesis and sister chromatid exchange during homologous recombination. Mol. Cell, **71**(1): 11–24.e17. doi:10.1016/j.molcel.2018.05.014.

Kepkay, R., Attwood, K.M., Ziv, Y., Shiloh, Y., and Dellaire, G. 2011. KAP1 depletion increases PML nuclear body number in concert with ultrastructural changes in chromatin. Cell Cycle, **10**(2): 308–322. doi:10.4161/cc.10.2.14551.

Lallemand-Breitenbach, V., and de The, H. 2010. PML nuclear bodies. Cold Spring Harb. Perspect. Biol. **2**(5): a000661. doi:10.1101/cshperspect.a000661.

Lallemand-Breitenbach, V., and de The, H. 2018. PML nuclear bodies: from architecture to function. Curr. Opin. Cell Biol. **52**: 154–161. doi:10.1016/j.ceb.2018.03.011.

Lemaitre, C., Grabarz, A., Tsouroula, K., Andronov, L., Furst, A., Pankotai, T., et al. 2014. Nuclear position dictates DNA repair pathway choice. Genes Dev. **28**(22): 2450–2463. doi:10.1101/gad.248369.114.

Li, C., Peng, Q., Wan, X., Sun, H., and Tang, J. 2017. C-terminal motifs in promyelocytic leukemia protein isoforms critically regulate PML nuclear body formation. J. Cell Sci. **130**(20): 3496–3506. doi:10.1242/jcs.202879.

Lundin, C., Erixon, K., Arnaudeau, C., Schultz, N., Jenssen, D., Meuth, M., et al. 2002. Different roles for nonhomologous end joining and homologous recombination following replication arrest in mammalian cells. Mol. Cell Biol. **22**(16): 5869–5878. PMID:12138197.

Mao, Z., Bozzella, M., Seluanov, A., and Gorbunova, V. 2008. DNA repair by nonhomologous end joining and homologous recombination during cell cycle in human cells. Cell Cycle, **7**(18): 2902–2906. doi:10.4161/cc.7.18.6679.

Munch, S., Weidtkamp-Peters, S., Klement, K., Grigaravicius, P., Monajembashi, S., Salomoni, P., et al. 2014. The tumor suppressor PML specifically accumulates at RPA/Rad51-containing DNA damage repair foci but is nonessential for DNA damage-induced fibroblast senescence. Mol. Cell Biol. **34**(10): 1733–1746. doi:10.1128/MCB.01345-13.

Nefkens, I., Negorev, D.G., Ishov, A.M., Michaelson, J.S., Yeh, E.T., Tanguay, R.M., et al. 2003. Heat shock and Cd2+ exposure regulate PML and Daxx release from ND10 by independent mechanisms that modify the induction of heat-shock proteins 70 and 25 differently. J. Cell Sci. **116**(Pt. 3): 513–524. PMID:12508112.

Negorev, D., and Maul, G.G. 2001. Cellular proteins localized at and interacting within ND10/PML nuclear bodies/PODs suggest functions of a nuclear depot. Oncogene, **20**(49): 7234–7242. doi:10.1038/sj.onc.1204764.

Orthwein, A., Noordermeer, S.M., Wilson, M.D., Landry, S., Enchev, R.I., Sherker, A., et al. 2015. A mechanism for the suppression of homologous recombination in G1 cells. Nature, **528**(7582): 422–426. doi:10.1038/nature16142.

Pierce, A.J., Johnson, R.D., Thompson, L.H., and Jasin, M. 1999. XRCC3 promotes homology-directed repair of DNA damage in mammalian cells. Genes Dev. **13**(20): 2633–2638. PMID:10541549.

Pierce, A.J., Hu, P., Han, M., Ellis, N., and Jasin, M. 2001. Ku DNA end-binding protein modulates homologous repair of double-strand breaks in mammalian cells. Genes Dev. **15**(24): 3237–3242. doi:10.1101/gad.946401.

Pinder, J., Salsman, J., and Dellaire, G. 2015. Nuclear domain 'knock-in' screen for the evaluation and identification of small molecule enhancers of CRISPR-based genome editing. Nucleic Acids Res. **43**(19): 9379–9392. doi:10.1093/nar/gkv993.

Postma, M., and Goedhart, J. 2019. PlotsOfData-A web app for visualizing data together with their summaries. PLoS Biol. **17**(3): e3000202. doi:10.1371/journal.pbio.3000202.

Richardson, C., Moynahan, M.E., and Jasin, M. 1998. Double-strand break repair by interchromosomal recombination: suppression of chromosomal translocations. Genes Dev. **12**(24): 3831–3842. PMID:9869637.

Rothkamm, K., Kruger, I., Thompson, L.H., and Lobrich, M. 2003. Pathways of DNA double-strand break repair during the mammalian cell cycle. Mol. Cell Biol. **23**(16): 5706–5715. PMID:12897142.

Salomoni, P., and Pandolfi, P.P. 2002. The role of PML in tumor suppression. Cell, **108**(2): 165–170. PMID:11832207.

Salsman, J., Stathakis, A., Parker, E., Chung, D., Anthes, L.E., Koskowich, K.L., et al. 2017. PML nuclear bodies contribute to the basal expression of the mTOR inhibitor DDIT4. Sci. Rep. **7**: 45038. doi:10.1038/srep45038.

Seker, H., Rubbi, C., Linke, S.P., Bowman, E.D., Garfield, S., Hansen, L., et al. 2003. UV-C-induced DNA damage leads to p53-dependent nuclear trafficking of PML. Oncogene, **22**(11): 1620–1628. doi:10.1038/sj.onc.1206140.

Shcherbakova, D.M., and Verkhusha, V.V. 2013. Near-infrared fluorescent proteins for multicolor in vivo imaging. Nat. Methods, **10**(8): 751–754. doi:10.1038/nmeth.2521.

Shen, T.H., Lin, H.K., Scaglioni, P.P., Yung, T.M., and Pandolfi, P.P. 2006. The mechanisms of PML-nuclear body formation. Mol. Cell, **24**(3): 331–339. doi:10.1016/j.molcel.2006.09.013.

Shiels, C., Islam, S.A., Vatcheva, R., Sasieni, P., Sternberg, M.J., Freemont, P.S., et al. 2001. PML bodies associate specifically with the MHC gene cluster in interphase nuclei. J. Cell Sci. **114**(Pt. 20): 3705–3716. PMID:11707522.

Trotman, L.C., Alimonti, A., Scaglioni, P.P., Koutcher, J.A., Cordon-Cardo, C., and Pandolfi, P.P. 2006. Identification of a tumour suppressor network opposing nuclear Akt function. Nature, **441**(7092): 523–527. doi:10.1038/nature04809.

van der Weyden, L., Adams, D.J., Harris, L.W., Tannahill, D., Arends, M.J., and Bradley, A. 2005. Null and conditional semaphorin 3B alleles using a flexible puroDeltatk loxP/FRT vector. Genesis, **41**(4): 171–178. doi:10.1002/gene.20111.

Vancurova, M., Hanzlikova, H., Knoblochova, L., Kosla, J., Majera, D., Mistrik, M., et al. 2019. PML nuclear bodies are recruited to persistent DNA damage lesions in an RNF168-53BP1 dependent manner and contribute to DNA repair. DNA Repair (Amst.), **78**: 114–127. doi:10.1016/j.dnarep.2019.04.001.

Wang, H., Xu, X., Nguyen, C.M., Liu, Y., Gao, Y., Lin, X., et al. 2018. CRISPR-mediated programmable 3D genome positioning and nuclear organization. Cell, **175**(5): 1405–1417.e1414. doi:10.1016/j.cell.2018.09.013.

Wang, Z.G., Delva, L., Gaboli, M., Rivi, R., Giorgio, M., Cordon-Cardo, C., et al. 1998. Role of PML in cell growth and the retinoic acid pathway. Science, **279**(5356): 1547–1551. PMID:9488655.

Weidtkamp-Peters, S., Lenser, T., Negorev, D., Gerstner, N., Hofmann, T.G., Schwanitz, G., et al. 2008. Dynamics of component exchange at PML nuclear bodies. J. Cell Sci. **121**(Pt. 16): 2731–2743. doi:10.1242/jcs.031922.

Wyman, C., and Kanaar, R. 2006. DNA double-strand break repair: all's well that ends well. Annu. Rev. Genet. **40**: 363–383. doi:10.1146/annurev.genet.40.110405.090451.

Yang, S., Kuo, C., Bisi, J.E., and Kim, M.K. 2002. PML-dependent apoptosis after DNA damage is regulated by the checkpoint kinase hCds1/Chk2. Nat. Cell Biol. **4**(11): 865–870. doi:10.1038/ncb869.

Yeung, P.L., Denissova, N.G., Nasello, C., Hakhverdyan, Z., Chen, J.D., and Brenneman, M.A. 2012. Promyelocytic leukemia nuclear bodies support a late step in DNA double-strand break repair by homologous recombination. J. Cell Biochem. **113**(5): 1787–1799. doi:10.1002/jcb.24050.

Zhong, S., Hu, P., Ye, T.Z., Stan, R., Ellis, N.A., and Pandolfi, P.P. 1999. A role for PML and the nuclear body in genomic stability. Oncogene, **18**(56): 7941–7947. doi:10.1038/sj.onc.1203367.